

Supporting Information

**Unraveling the Regulation of Polyhydroxy Electrolyte Additive for a Reversible,
Dendrite-Free Zinc Anode**

Cong Wang^{a,+}, Junming Hou^{b,+}, Yaping Gan^a, Lei Xie^a, Yi He^{a,*}, Qiang Hu^{b,*}, Shude Liu^{c, d},
Seong Chan Jun^{d,*}

^a Ecology and Health Institute, Hangzhou Vocational and Technical College, Hangzhou
310018, China

^b School of Materials and Energy, University of Electronic Science and Technology of China,
Chengdu 610054, China

^c JST-ERATO Yamauchi Materials Space-Tectonics Project, National Institute for Materials
Science, 1-1 Namiki, Tsukuba, Ibaraki, 305-0044 Japan

^d School of Mechanical Engineering, Yonsei University, Seoul, 120-749 South Korea

[+] These authors contribute equally to this work

*Corresponding Author. Email: heyi24@hzvtc.edu.cn (Y. He), huqiang@std.uestc.edu.cn (Q.
Hu), scj@yonsei.ac.kr (S. C.Jun)

Supplemental Experimental Details

Materials:

Zn foil (~0.1 mm) and Pt were purchased from Haoxuan Metal Material Co., Ltd. ZnSO₄·7H₂O (>99.0%), sucrose (TS, >99.9%), Ag/AgCl electrode, ammonium persulfate (APS, >99.99%) and V₂O₅ powder (>99.99%) were purchased from Sinopharm Chemical Reagent Co., Ltd. All other reagents were analytical grade and used directly without further purification. Deionized water was used to prepare all aqueous electrolytes.

Materials Characterization:

The micromorphology of the samples was observed using scanning electron microscopy (SEM, FEI-Quanta 250, USA). The elemental analysis of the samples was characterized using a scanning electron microscope (FE-SEM, JSM-7500, Japan) equipped with corresponding energy-dispersive X-ray (EDX) elemental mapping. The crystal structure of the samples was characterized through the X-ray diffraction analysis (XRD, Smart Lab, Rigaku, Japan) with Cu-K α (λ = 1.540598 Å, Smart Lab) source (scan rate of 4° min⁻¹) in the 2 θ range of 5°~85°. The analysis of the electrolytes was carried out by H magnetic resonance imaging (NMR spectroscopy (Bruker advance III) and Fourier transform infrared spectrum (FTIR, NICOLET iS50, USA).

Electrochemical Tests:

Electrochemical characterization of symmetrical Zn//Zn cells with two different electrolytes was conducted using both transparent cells and 2032-type coin cells. Electrochemical impedance spectroscopy (EIS) of these cells was conducted on an electrochemical workstation (CHI660E, Shanghai, China) over the frequency range of 100 kHz to 1 Hz. The Zn//V₂O₅ coin and pouch cells were galvanostatically charged/discharged in the voltage range of 0.2–1.5 V vs. Zn/Zn²⁺ at different current densities on a Land CT5001A battery tester, and specific capacities were calculated based on the active mass of V₂O₅ cathode. The mass of V₂O₅ and Zn foil are approximately 1.5 mg and 100 mg, respectively. The width of Zn, V₂O₅, and separator are 14 mm, 14 mm, and 18 mm, respectively. In addition, the amount of Suc-containing electrolyte used is 90 μ L.

Transparent Zn Cell and In Situ Dendrite Observation:

A transparent Zn-Zn cell was designed to observe the Zn dendrite growth. Specifically, a transparent glass dish, two Zn ribbons (0.5 cm × 3 cm), and two plastic clamps form a pool for observing the Zn dendrites. The transparent glass dish is used to store the electrolyte. The Zn dendrites growth was in situ observed by an optical microscope equipped with a digital camera. Meanwhile, the transparent Zn cell was tested for Zn stripping/plating using an electrochemical workstation (CHI660E).

Theoretical Calculations:

The Vienna ab initio simulation package (VASP) was used to perform all the calculations.^[1] The electronic exchange-correlation energy was implemented using the Perdew-Burke-Ernzerhof (PBE) functional within the generalized gradient approximation (GGA), and the projector augmented wave (PAW) method describing electron-ion interactions.^[2] In geometry optimization settings, the atomic positions were optimized until all components of the forces on each atom were less than -0.05 eV/\AA and the total energy converge was set to below 10^{-5} eV . The DFT-D3 correction was used to describe van der Waals interactions.^[3] A cutoff energy of 400 eV and a Monkhorst-Pack k-point grid of $2 \times 2 \times 1$ were used, respectively. A vacuum of 15 \AA was set to circumvent periodic interactions between the atoms.

The binding energy (E_b) is defined as

$$E_b = E_{A+B} - (E_A + E_B)$$

where E_{A+B} is the total energy of a combined system of A and B, $E_B + E_A$ is the sum of the total energies of A and B before the combination. A and B refer to Suc, Zn^{2+} , H_2O , and Zn slab (002), respectively.

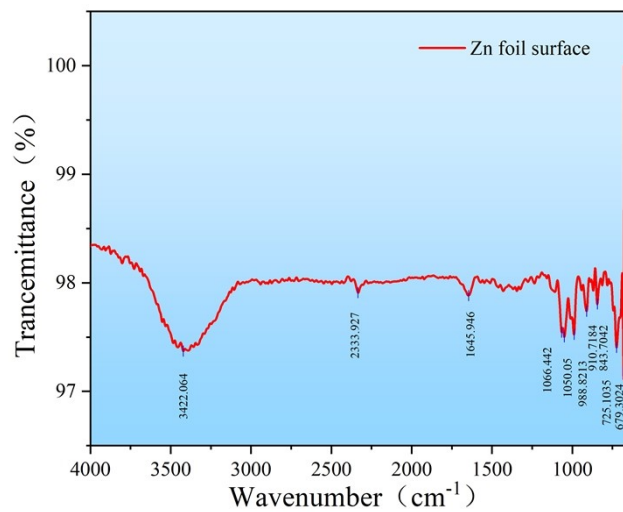


Fig. S1. FTIR spectrum of Zn foil soaked in 1 M ZnSO₄ with Suc after 1 day.

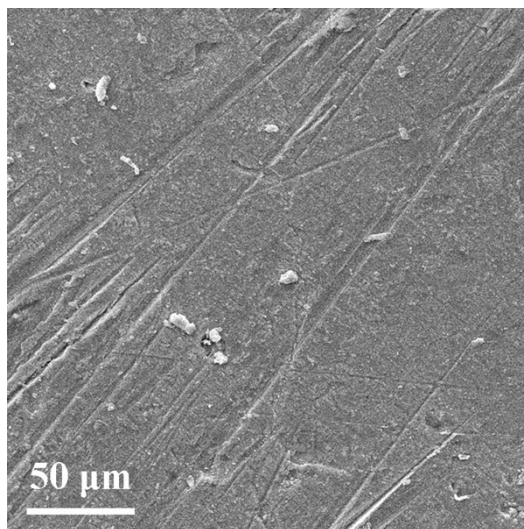


Fig. S2. SEM image of the pure Zn foil.

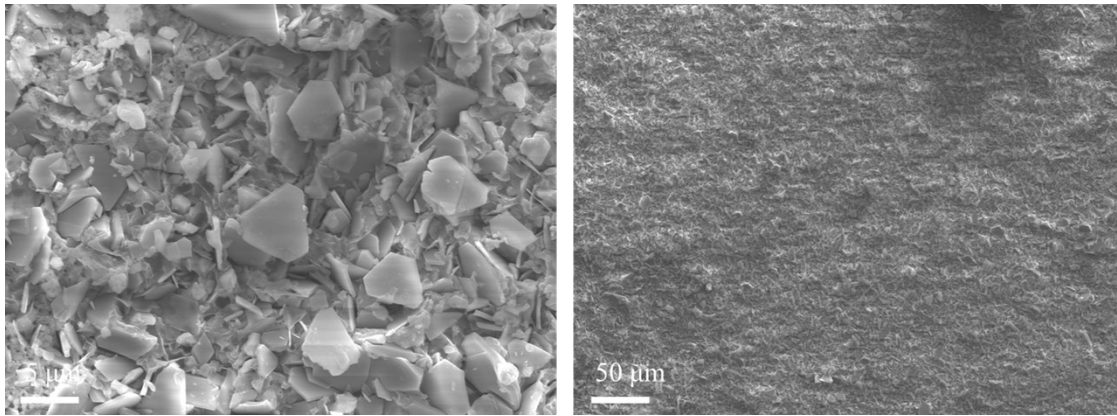


Fig. S3. SEM images at different magnifications for the Zn foil soaked in 1 M ZnSO₄ after 7 days.

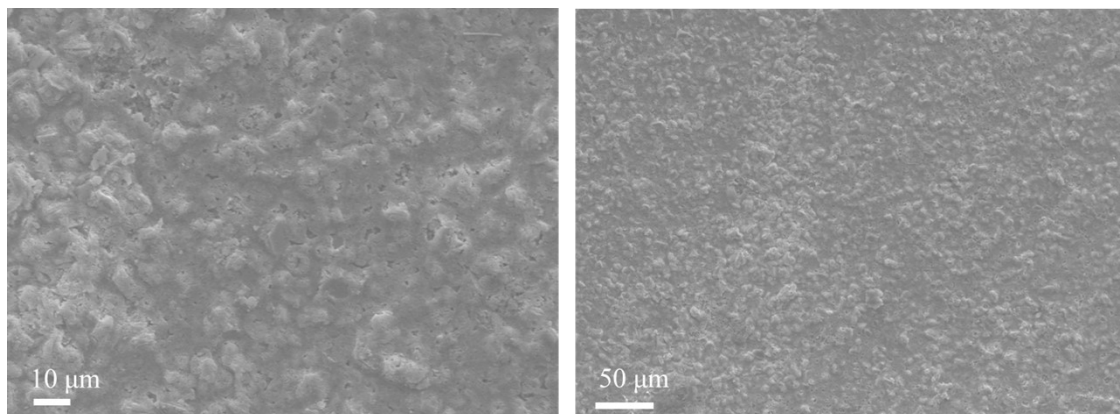


Fig. S4. SEM images at different magnifications for Zn foil soaked in 1 M ZnSO₄ with Suc after 7 days.

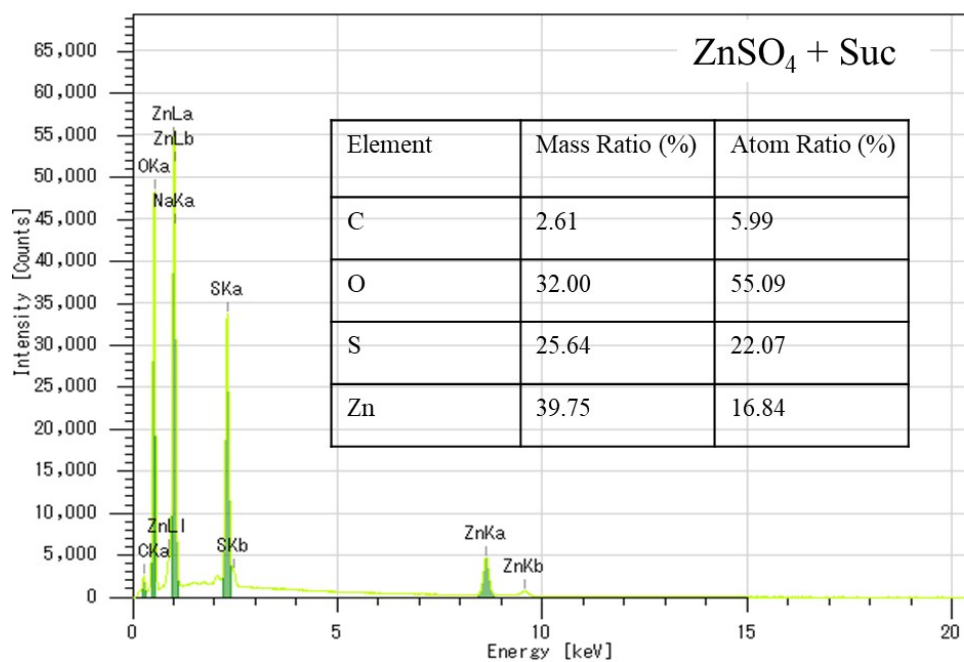


Fig. S5. EDS spectrum of Zn foil soaked in 1 M ZnSO₄ after 7 days.

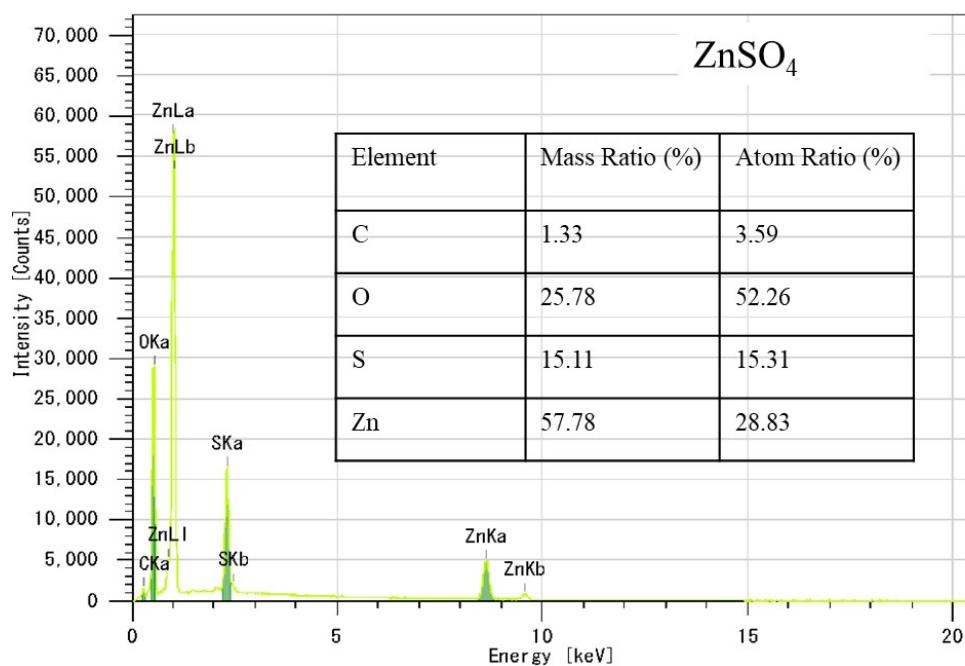


Fig. S6. EDS spectrum of Zn foil soaked in 1 M ZnSO₄ with Suc after 7 days.

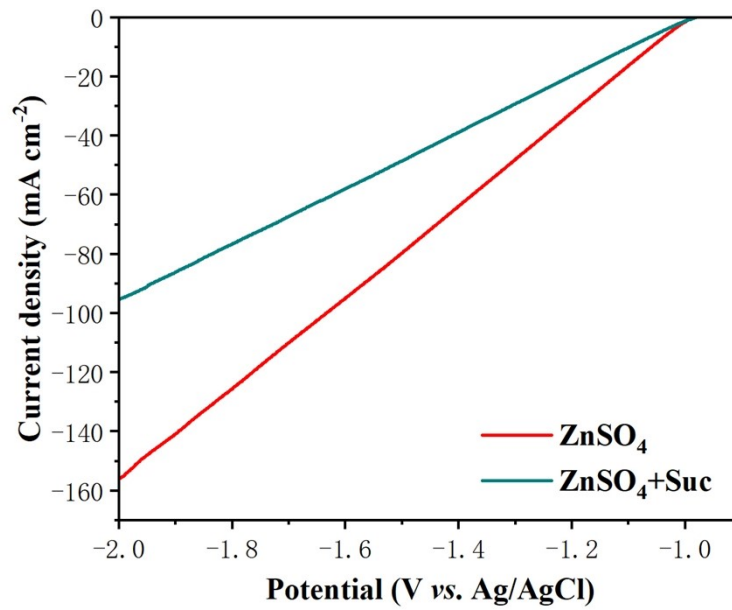


Fig. S7. Comparison of HER performance under ZnSO₄ and ZnSO₄ + Suc electrolyte systems.

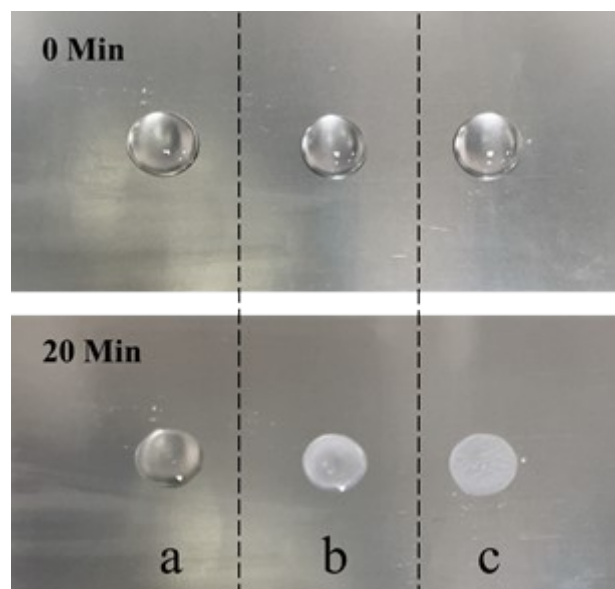


Fig. S8. Comparison of volatility among (a) 1 M Suc, (b) 1 M ZnSO₄ with 10 mM Suc, and (c) 1 M ZnSO₄ at room temperature.

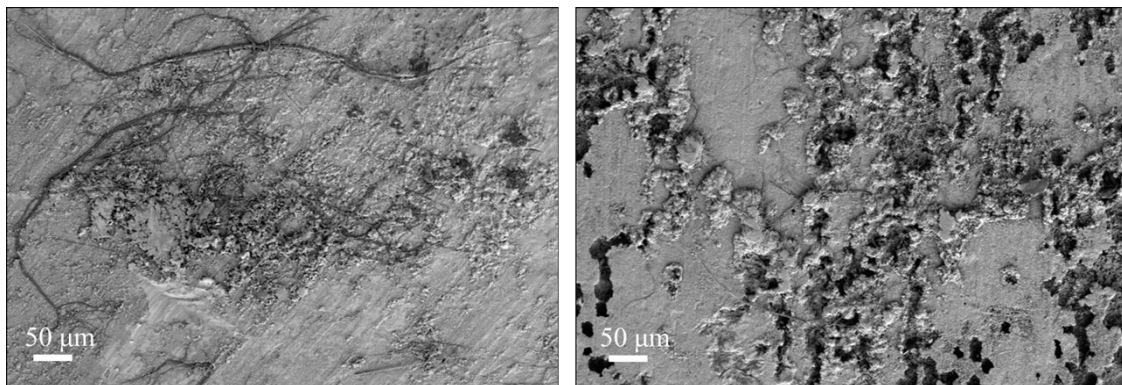


Fig. S9. SEM images of Zn electrodes that are cycled out of the cells in ZnSO₄ electrolyte after the 30th plating.

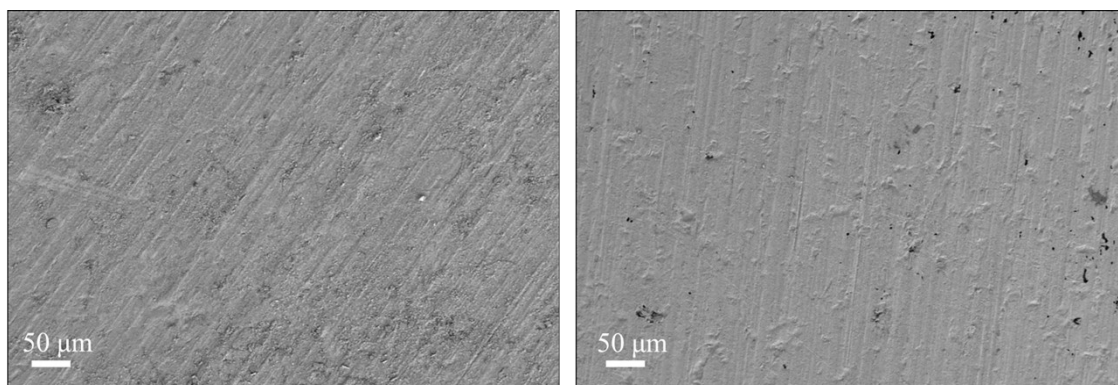


Fig. S10. SEM images of Zn electrodes cycled out of the cells in ZnSO₄ electrolyte with Suc after the 30th plating.

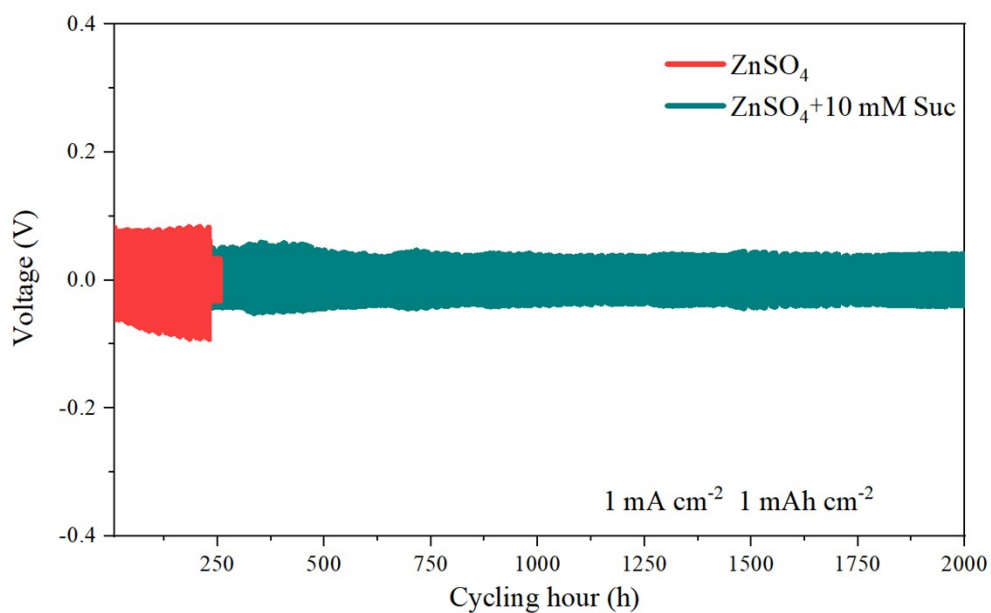


Fig. S11. Comparison of long-term galvanostatic charging/discharging of Zn//Zn symmetric cell between 1 M ZnSO₄ and 1 M ZnSO₄ with 10 mM Suc addition under a current density and deposition capacity of 1 mA cm⁻² and 1 mAh cm⁻², respectively.

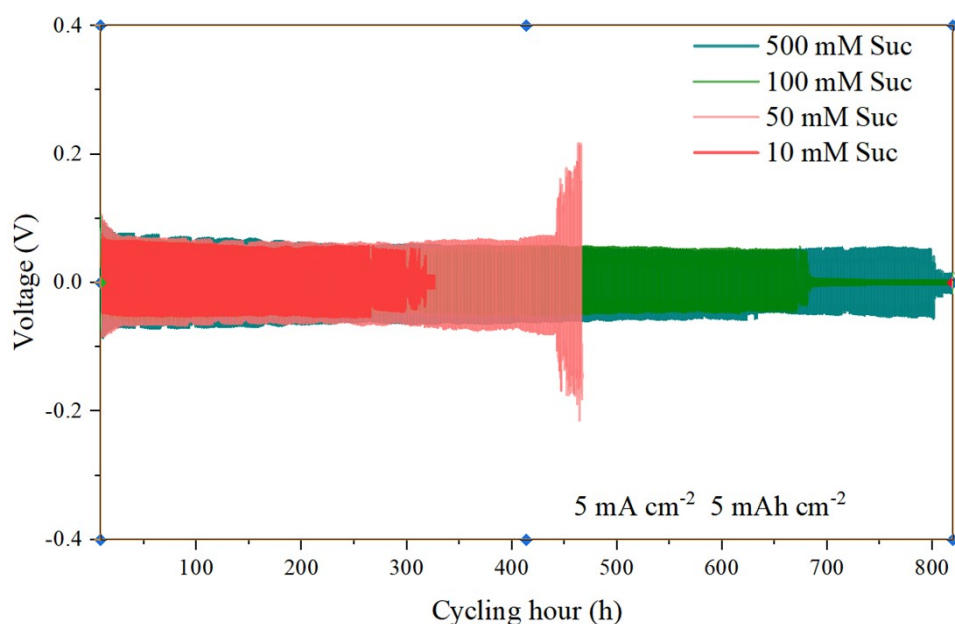


Fig. S12. Comparison of long-term galvanostatic charging/discharging of Zn//Zn symmetric cell with different Suc concentration addition under a current density and deposition capacity of 5 mA cm⁻² and 5 mAh cm⁻², respectively.

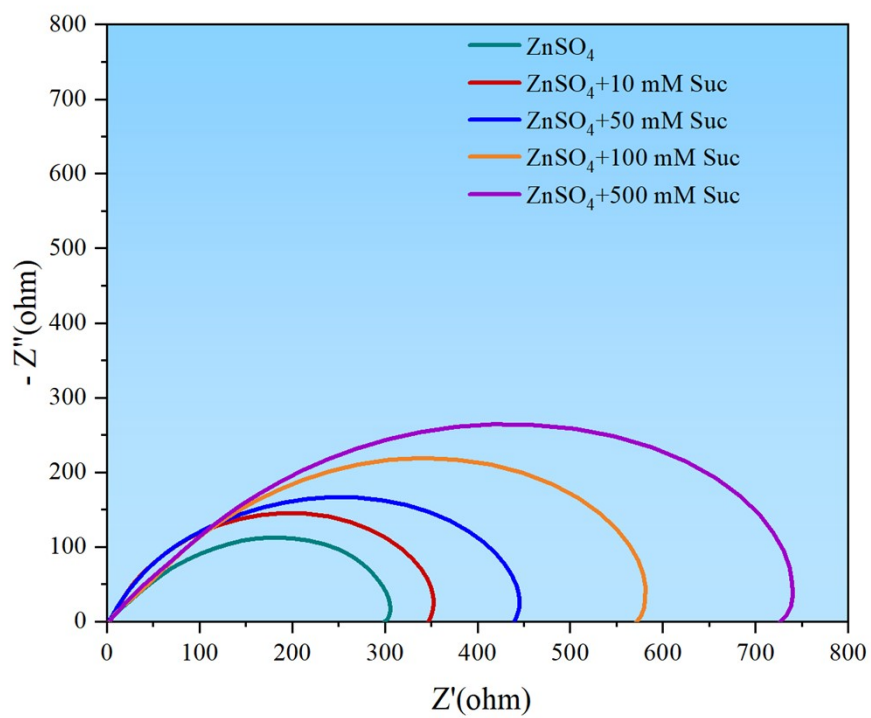


Fig. S13. Comparison of the electrochemical impedance of Zn//Zn symmetric cell in $ZnSO_4$ and $ZnSO_4$ with 10, 50, 100 and 500 mM electrolytes.

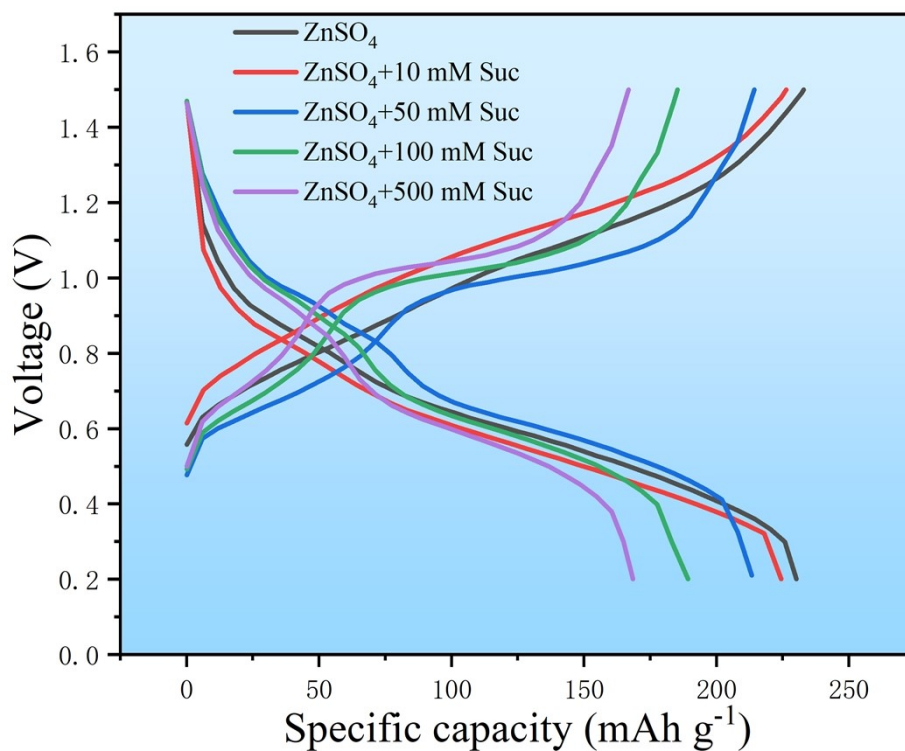


Fig. S14. Comparison of the specific capacity of Zn//V₂O₅ cells at a current density of 1 A g⁻¹ using ZnSO₄, and ZnSO₄ with 10, 50, 100 and 500 mM Suc electrolytes.

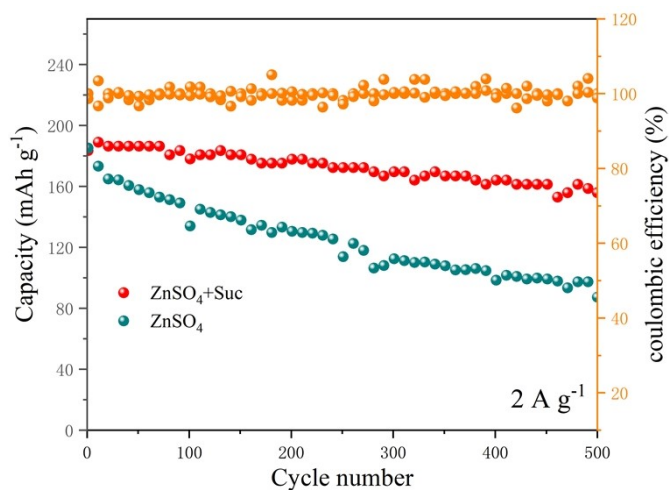


Fig. S15. Cycling performance of two Zn//MnO₂ coin cells at a current density of 2 A g⁻¹.

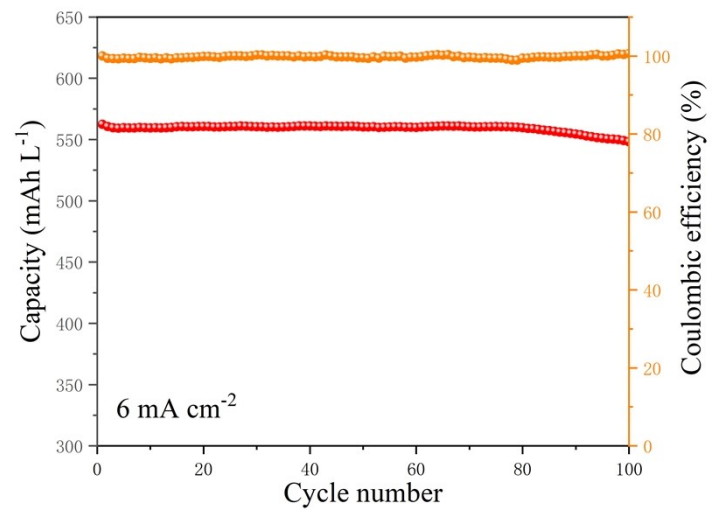


Fig. S16. Cycling performance of the Zn//V₂O₅ pouch battery under the current density of 6 mA cm⁻².

Table S1. Chemical cost estimation of reported electrolyte systems in ZIBs. (The cost is counted based on the price referred to Shanghai Aladdin Biochemical Technology Co., Ltd with all purity above 98%.)

Electrolyte type	Chemical	Aladdin catalog number (purity)	Mass required ($\text{g}\cdot\text{L}^{-1}$ electrolyte)	Unit Price ($\text{\$}\cdot\text{g}^{-1}$)	Total price ($\text{\$}\cdot\text{L}^{-1}$)	Reference
3 m ZnAc_2 + 3 m LiAc + 30 m KAc	ZnAc_2	Z110779 (99.99%)	550.44	0.455	1271.7	[4]
	LiAc	L118858 (99.99%)	197.97	0.697		
	KAc	P108329 (99%)	2944.2	0.300		
1 M $\text{Zn}(\text{TFSI})_2$ + 20 M LiTFSI	$\text{Zn}(\text{TFSI})_2$	Z299992 (98%)	625.65	3.962	16287.37	[5]
	LiTFSI	B398978 (99.9%)	5741.6	2.405		
30 m ZnCl_2	ZnCl_2	Z292534 (99.99%)	4089	6.724	27494.44	[6]
4.2 M ZnSO_4 + 0.1 M MnSO_4	ZnSO_4	Z111855 (99%)	1207.71	0.036	47.32	[7]
	MnSO_4	M111711 (99.99%)	16.91	0.227		
13 m ZnCl_2 + 0.8 m H_3PO_4	ZnCl_2	Z292534 (99.99%)	1771.9	6.724	12094.34	[8]
	H_3PO_4	P120547 (99%)	78.4	2.297		
67% Maltose + 2 M ZnSO_4	Maltose	M104816 (98%)	670	0.102	75.17	[9]
	ZnSO_4	Z111855 (99%)	189.78	0.036		
32 vol% 3 M ZnSO_4 + 68 vol% EG	Ethylene glycol	E119700 (99.8%)	756.84	0.163	133.30	[10]
	ZnSO_4	Z111855 (99%)	276.06	0.036		
10 m M Sucrose + 1 M ZnSO_4	Sucrose	S112226 (99.9%)	3.42	0.063	10.57	This work
	ZnSO_4	Z111855 (99%)	287.56	0.036		

Table S2. Comparison of high current stability performance of ZIBs from previous reports and our work.

Cathode	Electrolyte	Cycling condition		Capacity retention	Reference
		Current (A·g ⁻¹)	Cycle number		
HfO ₂ -coated ZVO	1 M ZnSO ₄	10	1000	84%	[11]
V ₂ O ₅	1 M Zn(CF ₃ SO ₃) ₂	5	1000	99.3%	[12]
NaCa _{0.6} V ₆ O ₁₆ ·3H ₂ O	3 M Zn(CF ₃ SO ₃) ₂	2	2000	94%	[13]
VO ₂	1 M ZnSO ₄	3	945	75.5%	[14]
H ₂ V ₃ O ₈	3 M Zn(CF ₃ SO ₃) ₂	20	2000	87%	[15]
Fe ₅ V ₁₅ O ₃₉ (OH) ₉ ·9H ₂ O	1 M ZnSO ₄	5	300	80%	[16]
α-MnO ₂	1 M ZnSO ₄	2.5	100	100%	[17]
V ₂ O ₅	3 M ZnSO ₄	2	400	93.4%	[18]
MnO ₂	10 m M Glucose + 1 M ZnSO ₄	3.08	1000	80%	[19]
MnO ₂	2 M ZnSO ₄	1	900	83.1%	[20]
V ₂ O ₅	10 m M Sucrose + 1 M ZnSO ₄	10 A·g ⁻¹	2000	96.2%	This work

References:

- [1] G. Kresse, J. Hafner, *Phys Rev B Condens Matter*. **1993**, *47*, 558 – 561.
- [2] J. P. Perdew, K. Burke, Ernzerhof M, *Phys Rev Lett*. **1996**, *77*, 3865 – 3868.
- [3] S. Grimme, J. Antony, S. Ehrlich, H. Krieg, *J Chem Phys*. **2010**, *132*, 154104.
- [4] J. Han, A. Mariani, A. Varzi and S. Passerini, *J. Power Sources*. **2021**, *485*, 229329.
- [5] F. Wang, O. Borodin, T. Gao, X. Fan, W. Sun, F. Han, A. Faraone, J. Dura, K. Xu and C. Wang, *Nat. Mater*. **2018**, *17*, 543.
- [6] C. Zhang, J. Holoubek, X. Wu, A. Daniyar, L. Zhu, C. Chen, D. P. Leonard, I. A. Rodriguez- Perez, J. X. Jiang, C. Fang and X. Ji, *Chem. Commun*. **2018**, *54*, 14097 – 14099.
- [7] B. Olbasa, F.. Fenta, S. Chiu, M. Tsai, C. Huang, B. Jote, T. Beyene, Y. Liao, C. Wang, W. Su, H. Dai and B. H wang, *ACS Appl. Energy Mater*. **2020**, *3*, 4499 – 4508.
- [8] H. Shi, Y. Song, Z. Qin, C. Li, D. Guo, X. Liu and X. Sun, *Angew. Chem. Int. Ed*. **2019**, *58*, 16057-16061.
- [9] W. Chen, S. Guo, L. Qin, L. Li, X. Cao, J. Zhou, Z. Luo, G. Fang and S. Liang, *Adv. Funct. Mater*. **2022**, 2112609.
- [10] R. Qin, Y. Wang, M. Zhang, Y. Wang, S. Ding , A. Song , H. Yi , L. Yang , Y. Song , Y. Cui , J. Liu , Z. Wang , S. Li, Q. Zhao, F. Pan, *Nano Energy*. **2021**, *80*, 105478.
- [11] J. Guo, J. Ming, Y. Lei, W. Zhang, C. Xia, Y. Cui and H. N. Alshareef, *ACS Energy Lett*. **2019**, *4*, 2776 – 2781.
- [12] N. Zhang, Y. Dong, M. Jia, X. Bian, Y. Wang, M. Qiu, J. Xu, Y. Liu, L. Jiao and F. Cheng, *ACS Energy Lett*. **2018**, *3*, 1366 – 1372.

- [13] K. Zhu, T. Wu, K. Huang, *Adv. Energy Mater.* **2019**, *9*, 1901968.
- [14] Z. Li, S. Ganapathy, Y. Xu, Z. Zhou, M. Sarilar and M. Wagemaker, *Adv. Energy Mater.* **2019**, *9*, 1900237.
- [15] Q. Pang, C. Sun, Y. Yu, K. Zhao, Z. Zhang, P. Voyles, G. Chen, Y. Wei and X. Wang, *Adv. Energy Mater.* **2018**, *8*, 1800144.
- [16] Z. Peng, Q. Wei, S. Tan, P. He, W. Luo, Q. An and L. Mai, *Chem. Commun.* **2018**, *54*, 4041 – 4044.
- [17] C. Xu, B. Li, H. Du and F. Kang, *Angew. Chem. Int. Ed.* **2012**, *51*, 933 – 935.
- [18] J. Zhou, L. Shan, Z. Wu, X. Guo, G. Fanga and S. Liang, *Chem. Commun.* **2018**, *54*, 4457 – 4460.
- [19] P. Sun, L. Ma, W. Zhou, M. Qiu, Z. Wang, D. Chao and W. Mai, *Angew. Chem. Int. Ed.* **2021**, *60*, 18247– 18255.
- [20] W. Guo, Y. Zhang, X. Tong, X. Wang, L. Zhang, X. Xia, J. Tu, *Materials Today Energy.* **2021**, *20*, 100675.